

The impacts of post-wildfire on streamflow and sediment dynamic in Mae Chaem River Basin

Prangtip Triritthiwittaya^{1,*}, Chaiwat Ekkawatpanit^{1,*}, Duangrudee Kositgittiwong¹ and Amnat Chidthaisong²

¹Department of Civil Engineering, Faculty of Engineering, King Mongkut's University of Technology Thonburi, 126 Prachauthit Rd., Bangmod, Tungkru, Bangkok 10140, Thailand

²The Joint Graduate School of Energy and Environment, King Mongkut's University of Technology Thonburi, 126 Prachauthit Rd., Bangmod, Tungkru, Bangkok 10140, Thailand

*Corresponding author: prangtip.t@mail.kmutt.ac.th; chaiwat.ekk@kmutt.ac.th

Abstract: The Mae Chaem River Basin experienced frequent wildfires, particularly during the dry season (January to April), with the majority occurring in reserved forest areas. These wildfires' impact is generally classified by severity, disrupted vegetation, soil properties, and hydrological regimes. This study aims to evaluate streamflow and sediment dynamics changes from 2014 to 2018 using the Soil and Water Assessment Tool (SWAT), comparing pre-fire and post-fire scenarios. The results from the Difference Normalized Burn Ratio (dNBR) showed that low severity burn areas, comprising 20-67% of the total burned area, led to an escalation of peak discharge and sediment flow during the rainy season (May to September). The study found that the total runoff increased by 3% after the fire, which indicates a potential for more severe flooding. The average annual baseflow increased at the basin scale but fluctuated at the subbasin scale. The influence of wildfires on sediment transport exhibited a heightened magnitude compared to water yield. The sediment outflow from the watershed increased by approximately 15% based on the post-fire model. This increase was found to be related to precipitation intensity and the proportion of the burned area. Furthermore, sediment degradation and deposition were found to shift towards subbasins, with 25% of burned areas becoming more susceptible to combustion.

Keywords: Burned area, sediment dynamic, streamflow, SWAT, wildfire.

1. Introduction

Wildfires are unpredictable disasters that frequently occur in the northern region of Thailand. They have significant immediate and prolonged effects on the dynamic patterns of natural components such as land, water, soil, and weather [1-3]. These wildfires mainly occur on typical steep slopes. Despite the apparent evidence of forest fires in Thailand, statistical data on burned areas is rarely found in terms of spatial and temporal distribution. Conducting burn scar assessments is necessary to understand the effects of wildfires for the recovery plan. The severity of the burn area is related to the magnitude of the fire-induced deterioration of vegetation. Several indices are commonly used in the archived satellite imageries in academic research to assess burn severity from wildfires, such as the Normalized Burn Index (NBI), the Difference Normalized Burn Ratio (dNBR), the Composite Burn Index (CBI), and the Burned Area Reflectance Classification (BARC) [4]. These indices are calculated using various spectral bands, vegetation indices, and topographic information. The extent and severity of burn damage caused by wildfires and the recovery of vegetation in the aftermath can be assessed using satellite imagery, which is considered a valuable tool. However, it must be acknowledged that various factors, such as the quality of input data, the spatial and temporal resolution of images, and the unique characteristics of the wildfire, can influence the accuracy of these assessments. Indices for assessing burn damage can be provided by various satellite systems, such as Landsat 5-8, MODIS, Sentinel-2, and Sentinel-1. Furthermore, the accuracy of the burn area indices obtained from these systems can also be affected by factors such

as data quality, image resolution, and wildfire characteristics. In this study, the advantage of the NBR index is utilized to identify the burned scars, which can detect subtle differences in vegetation reflectance using satellite or aerial imagery from Landsat-7. Burn severity classification was calculated by the Difference Normalized Burn Ratio (dNBR) from satellite images, highlighting burned areas in forest zones.

In addition, the stability of the hydrological system and land characteristics are immediately altered when a forest basin is disrupted by wildfire. As such, the impact of wildfires on hydrological changes and soil surface erosion is currently being widely studied by global societies in order to better understand the responsibilities associated with these phenomena [5]. The reduction in vegetation density leads to less infiltration and more overland flow, which can increase the amount of sediment transported to streams and rivers. The erosion can also cause changes to the channel morphology and sediment transport patterns [6-7]. With the loss of protective plant cover, the soil surface becomes exposed to the force of raindrops, which increases the risk of flash floods, particularly during the rainy season [8]. The peak discharges were possibly accelerated by a higher velocity of surface runoff [9-10]. The minimum flow of water that controls the health of streams and is also sustained by groundwater discharge is known as "baseflow or low-flow". The impact of wildfires on baseflow low-flow that generally occurs during drought or low precipitation can vary, with some studies observing an increase in low-flow, while others have reported a decline depending on the severity of the fire and the proportion of burned areas [11]. Consequently, wildfires devastated the landform and shaped a new ecological system within the territorial catchment.

Wildfires can have a significant impact on soil erosion and the dynamics of sediment transport. High temperatures can cause thermal erosion and the removal of vegetation, which can increase surface runoff and fluvial erosion, leading to incremental sediment transport downstream. The deposited and eroded soil particles inevitably have an inherent connectivity with surface runoff and dynamic mobility along river channels [12]. This connectivity depends on the circulation of sediment particles through the channel tributaries. The higher rate of erosive soil has led to the degradation of land and channels. Considering wildfire impact, land use and land cover (LULC) have been permanently changed due to the removal of vegetation cover. Soil properties may change due to the heat from the wildfire, varying with the temperature, burning duration and severity of the wildfire [13]. Wildfires significantly reduce soil moisture, remove organic matter, and deteriorate soil structure and porosity [14]. Additionally, the heat from a wildfire can cause changes to the soil's properties, making it less able to retain water and more susceptible to erosion. This can lead to increased sediment loads in streams and rivers, which can cause problems for downstream water users.

Hydrological models that are used to estimate flow rates and sediment yields must be able to change these relevant parameters. Therefore, integrating the estimated combustion map into the hydrological system is a complex and spatially variable process in some particular catchments. Frequently used hydrological models for simulating streamflow after a wildfire include the Distributed Hydrology Soil Vegetation Model (DHSVM), the Precipitation Runoff Modeling System (PRMS), the Soil and Water Assessment Tool (SWAT), and models based on Hydrological Response Units (HRUs). The Soil and Water Assessment Tool (SWAT) is utilized to conduct a comprehensive analysis of the hydrological system and sediment dynamics within the context of fire conditions. Its capability to adjust parameters related to land use and land cover characteristics is a key feature of the tool to compare pre-fire and post-fire modeling according to burned severity levels [15].

The impacts of wildfires are pervasive on a global scale. A number of nations that have been beset by severe wildfires, such as the United States and Australia, have a vested interest in investigating the immediate and prolonged hydrological response on their respective ecosystems. However, in Thailand, there has been a paucity of research conducted on the hydrological and sedimentation responses after forest fires. The distributed hydrological model, known as the SWAT model, has been utilized in this study to evaluate daily discharge and sediment changes in the Mae Chaem River basin between pre-fire and post-fire conditions in the years 2014 to 2018. The objectives of this study are to: (1) assess variations in streamflow characteristics, specifically focusing on surface runoff and baseflow, and (2) examine the dynamics of sediment particles along the Mae Chaem River. The evaluation of streamflow and sediment dynamics have been analyzed under pre-fire and post-fire conditions.

2. Methods and Materials

2.1 Study area

About 90% of the watershed is located in Mae Chaem, Chiang Mai. The southwestern basin covers the regions of Mae La Noi and Mae Hong Son. It has been designated as a class 1A area where the forested area has never been disturbed by human impact. The majority of the basin area is covered by evergreen and deciduous forests with diverse vegetation. It has been preserved as headwater by the government, and is officially recognized as the Mae Chaem National Reserved Forest. The drainage area of the basin encompasses 3,909 km². The length of the river within its bounds is 207.2 km, and it is situated at an altitude of 650 meters above the mean sea level [16]. In this study, the basin

was divided into 12 subbasins. The area of each subbasin ranges from 56.05 to 500.38 km², and the slope gradient ranges from 1.24% to 53.88%. The Thai Meteorological Department reported that the climate in the basin was characterized by a yearly rainy season starting in May and ending in October, while the dry season spans from January to April [17]. The annual average accumulated rainfall is 970 mm, with the annual maximum and minimum temperatures being 24°C and 14°C, respectively [16]. The monitoring of the upper stream discharge was conducted at Ban Kong Kan, Mae Suk, Mae Chaem, where the designated inlet station (061302) was situated. The outlet station, labelled P.14A, is positioned in Ban Tha Kham, Hong Dong, Hod and is depicted in Figure 1. Additionally, the measurement of sediment concentration was obtained at inlet station 061302.

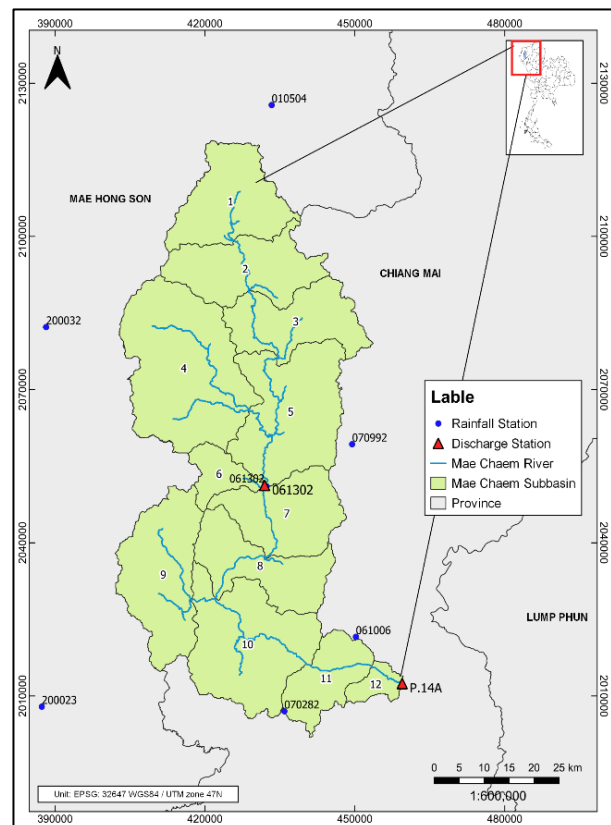


Figure 1. The study region encompasses 12 subbasins, with boundaries crossing two provinces (Mae Hong Son and Chiang Mai). The station 061302 and P.14A were established as inlet and outlet hydrometric stations to measure water flow, respectively.

2.2 Temporal Forest Fire

Wildfires are a recurrent problem in northern Thailand, especially during the dry season, which exacerbates the region's air quality crisis. To mitigate this situation, the Geo-Informatics and Space Technology Development Agency (GISTDA) utilizes satellite imagery to detect the locations of hotspots within Thailand. This study utilized the MODIS hotspot from FIRMS to delineate the study area, finding the highest cumulative historical hotspot between 2010 and 2021. Numerous reports indicate that hotspots were detected primarily in Chiang Mai, with a secondary occurrence in Mae Hong Son. The most critical region with the highest accumulation of hotspots over the past decade was found to be the Mae Chaem district, where a maximum of 4,817 points were recorded, with the largest concentration appearing in the Mae Suk subdistrict. The majority of hotspots are clustered in the reserved forest area because some tropical-forest root-crop farmers encroach on the forest area for agriculture, like corn

fields. This method is called “slash-and-burn agriculture”. The average burning severity in the forest areas of the Mae Chaem River Basin was low. The vegetation restoration map in Figure 2 was analyzed using the Normalized Difference Vegetation Index (NDVI) to measure the leafiness and health of the vegetation [18]. The temporal scenarios of post-fire conditions were evaluated one year after the fire occurrence (2014 to 2018). The post-fire models were prevented from vegetation regrowth and no post-fire mitigation activities were conducted during the assessment.

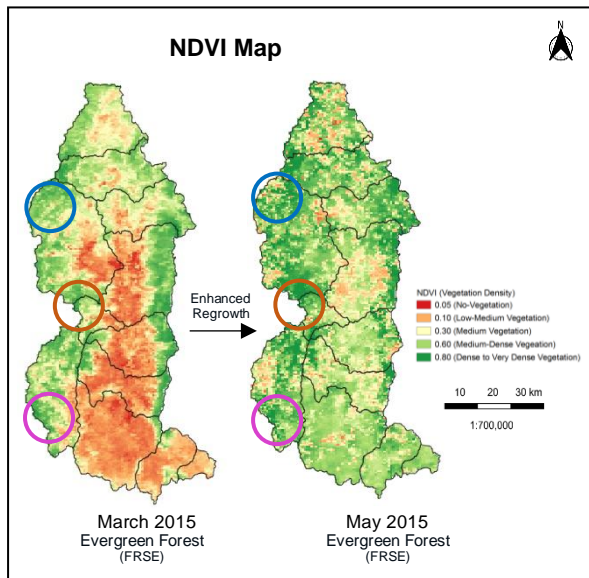


Figure 2. The example of Normalized difference vegetation index (NDVI) images on March and May. As the label description in the map, the red and green zones adversely represent the vegetation health. The circles cropped the mitigation from wildfire in the evergreen forest zone.

2.3 Fire Burn Severity Assessment

The Burn Indices method, integrated with the QGIS program, was utilized to estimate burn scars in the Mae Chaem River Basin. The burned maps, assessed in this study from 2014 to 2018, are satellite products from Landsat 7 ETM+ surface reflectance with a resolution of 30 m. The assessments provide information on damage extent, affected areas, severity of burn, and affected vegetation. This helped identify high priority areas and aid recovery planning, monitor post-fire recovery, including vegetation regrowth, soil changes and new habitats, and identify areas of high ecological value that need special protection during recovery. The satellite imagery utilized in the present study was selected with minimal cloud masking, with the images chosen to present the pre-fire scenario being procured in January, and those selected to depict the post-fire situation being obtained during the latter part of April.

2.3.1 Normalized Burn Ratio (NBR)

The Normalized Burn Ratio (NBR) is a uniquely formulated index with the purpose of identifying burned areas. The NBR is expressed mathematically using a formula that correlates near-infrared (NIR) and short-wave infrared (SWIR) bands, as depicted in Equation 1. The NBR values differentiate healthy vegetation from burned areas, with high NIR/low SWIR indicating healthy vegetation, and negative NBR indicating areas affected by fire and now bare soil [19]. A positive NBR suggests healthy vegetation, while a low NBR indicates recent burning and barrenness. Unburned areas have near-zero NBR values.

$$NBR = \frac{(NIR - SWIR)}{(NIR + SWIR)} \tag{1}$$

In Landsat-7, NIR is Near Infrared or Band 4 and SWIR is Short Wave Infrared or Band 7.

2.3.2 Difference Normalized Burn Ratio (dNBR)

The severity of wildfire can differ based on the ecosystem and is commonly evaluated through the loss of vegetation. In the current study, the burn severity was determined by examining the NBR difference between pre-fire and post-fire conditions [20]. A higher value of dNBR indicates more severe damage; whereas, the area with a negative dNBR value shows enhanced regrowth after the fire.

$$dNBR = NBR_{pre-fire} - NBR_{post-fire} \tag{2}$$

2.3.3 Burn Severity Threshold

After NBR images have been calculated by Equation 1. The criteria to highlight a pixel that is expressed as a burning area must achieve two statistical requirements [21]:

- Condition 1: If NBR of post-fire $\leq \alpha$
- Condition 2: If $dNBR \geq \beta$

The α is the threshold for NBR after burning and the β is the threshold for the change of NBR. The value of α is obtained based on $\mu + 2\sigma$ of the NBR post-fire image and the value of β is also calculated based on $\mu - 2\sigma$ of the dNBR images. Thus, μ is the average value of NBR from total post-fire images, σ is the standard deviation of the dNBR value from total dNBR images. Based on the threshold analysis, the fire severity was classified into three levels as shown in Table 1, emphasized by the spatial response [21]. The observation of the burned area was available only in the protected forest area, which is under the supervision of the 16th Conservation Area Administration Office, National Park Division, Department of National Park, Wildlife and Plant Conservation [22]. The burn severity criterion is used similarly to calculate the combustion area for the total watershed area. The burned severity maps are illustrated in Figure 3.

Table 1. Fire Severity Classification.

Severity Level	Condition
Low	$\mu + 2\sigma \leq dNBR \leq \mu - 1\sigma$
Moderate	$\mu + 2\sigma \leq dNBR < \mu$
High	$dNBR \geq \mu$

2.4 Conceptualization of SWAT Model

The SWAT is a semi-distributed model developed to simulate rainfall-runoff, evapotranspiration and subsurface flow characteristics of a basin. The smallest parts of the models were generated from digital elevation (DEM), LULC, soil type and weather data [15, 23]. The multiple HRUs function is used to separate 5% of slope, soil, and LULC to optimize models and discard insignificant HRUs as show in Figure 4. After SWAT modelling was accomplished, the streamflow, and sediment transportation and dynamics were evaluated further. The calibration and validation of the pre-fire model must be accepted as an effective model based on R² and NSE values. The vital input for the SWAT model, as depicted in Figure 5, has been presented. The SWAT model, when paired with burned area data, can simulate the effects of wildfire on hydrological processes and water resources. The estimation of changes in vegetation, biomass, and soil properties from wildfires is based on data including severity maps and updated land use and land cover information in the model. The post-fire conditions were assessed based on climatic-hydrological basin factors and channel properties. The parameters of channel properties remained at the same optimal value from pre-fire condition, which are the Muskingum calibrated coefficients (MSK_CO1, MSK_CO2, and MSK_X), the fraction of transmission losses (TRNSRCH), the Reach evaporation adjustment factor (EVRCH), and the Manning’s “n” value for main channel (CH_N2), and the effective

hydraulic conductivity in main channel alluvium (CH_K2). However, the characteristics of LULC and optimal values of effective related parameters, such as the maximum canopy storage (CANMX), the initial SCS runoff curve number of moisture condition II (CN2), the soil evaporation compensation

factor (ESCO), and the plant uptake compensation factor (EPCO) were adjusted for post-fire modelling during 2014-2018. The annual burning maps were combined to examine the streamflow and sediment dynamics within each year. The hierarchical procedure utilized in the study is shown in Figure 5.

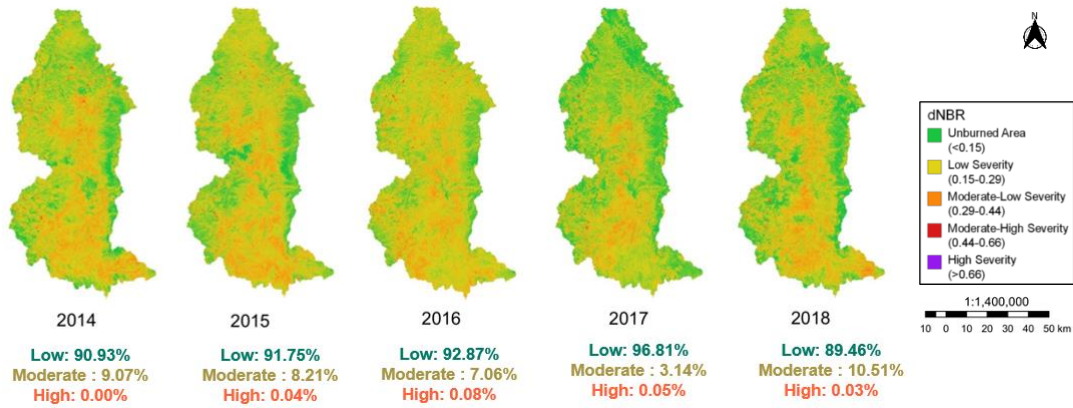


Figure 3. The map depicts the severity of fires from 2014 to 2018, as assessed by Landsat-7 Surface Reflectance and validated with data from the National Park Division's 16th Conservation Area Administration Office.

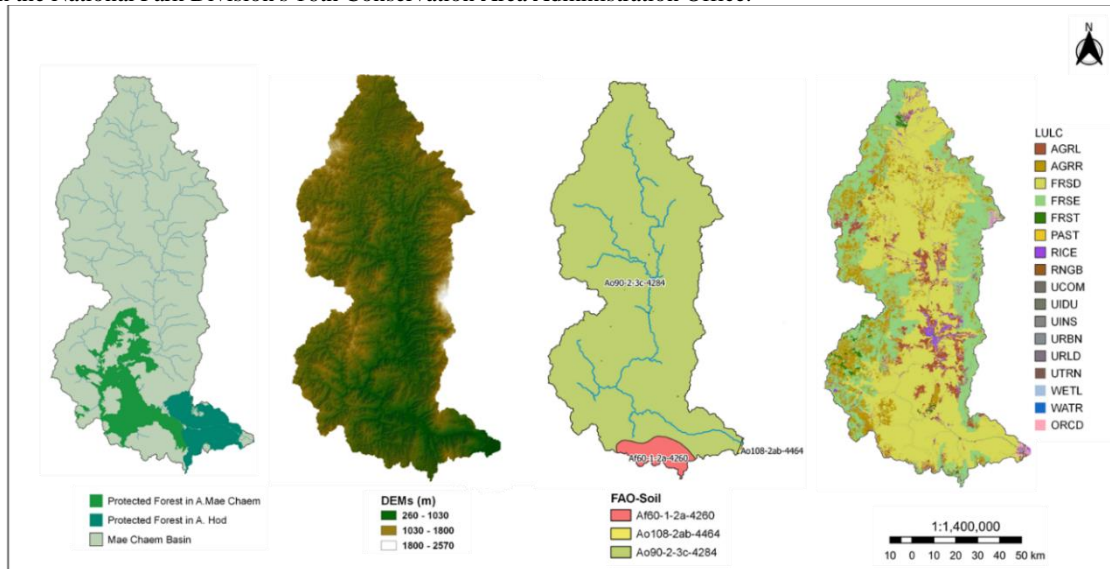


Figure 4. Conservation Forest Area and the secondary data for Mae Chaem River Basin consist of Digital Elevation from Shuttle Radar Topography Mission (SRTM), LULC from Land Development Department (LDD) where the light green is deciduous forest and the dark green is evergreen forest, and Soil map from Food and Agriculture Organization (FAO).

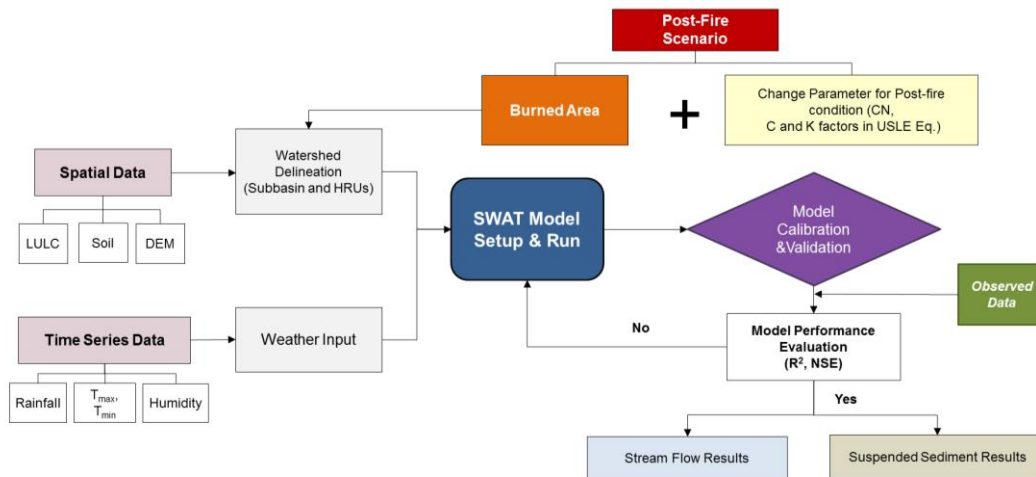


Figure 5. The overall flowchart illustrates the consequences and conceptual model in this study.

2.4.1 Runoff Simulation

Similar to other hydrological models, the SWAT model is mainly driven by the water balance equation (Equation 3) in hydrological processes. For SWAT analysis, two main approaches are available. Firstly, the land phase of the hydrological system, which includes the amount of water surface, sediment, nutrients, and pesticide loading. The routing phase, which can be defined by the channel properties from the headwater to the downstream, is the second division [23].

$$SW_t = SW_0 + \sum_{i=1}^t (R_{day} - Q_{surf} - E_a - W_{seep} - Q_{gw}) \quad (3)$$

where: SW_t is the final soil water content (mm), SW_0 is the initial soil water content (mm), t is the time (days), R_{day} is the amount of precipitation (mm), Q_{surf} is the amount of surface runoff (mm), E_a is the amount of evapotranspiration (mm), W_{seep} is the amount of water entering the vadose from the soil profile (mm), and Q_{gw} is the amount of return flow (mm).

Surface runoff is the precipitation runoff that excesses over the ground surface when the soil is saturated beyond the rate of infiltration [24]. The runoff volume was calculated empirically using the general SCS curve number as shown in the equation below [25].

$$Q_{surf} = \frac{(R_{day} - I_a)^2}{(R_{day} - I_a + S)} \quad (4)$$

where: Q_{surf} is the accumulated runoff or rainfall excess i (mm), R_{day} is the rainfall depth for the day (mm), I_a is the initial abstractions which includes surface storage, interception and infiltration prior to runoff (mm), and S is the retention parameter (mm).

2.4.2 Sediment Simulation

The SWAT utilizes the Universal Soil Loss Equation (USLE), developed by Wischmeier and Smith [23, 26], to evaluate the soil erosion in HRUs. The USLE equation enables to calculate the erosive energy of runoff based on rainfall intensity. The sediment yield was calculated based on Equation 5.

$$sed = 11.8 (Q_{surf} q_{peak} area_{hru})^{0.56} K_{USLE} \times P_{USLE} \times LS_{USLE} \times CFRG \quad (5)$$

where: sed is the sediment yield on given day (metric tons), Q_{surf} is the surface runoff volume (mm /ha), q_{peak} is the peak runoff rate (m^3/s), $area_{hru}$ is the area of the HRU (ha), K_{USLE} is the soil erodibility factor, C_{USLE} is the USLE cover and management factor, P_{USLE} is the USLE support practice factor, LS_{USLE} is the USLE topographic factor, and $CFRG$ is the coarse fragment factor.

The simulation of sediment transport was regulated by the interplay of two processes, i.e., degradation and deposition. Degradation and deposition in the main channels were determined by combining stream power, channel slope, and peak channel velocity using Bagnold's equation [27].

$$q = c \frac{\rho}{g} \sqrt{\frac{d}{D}} u_*^3 \quad (6)$$

where: q is the mass transport of sediment across a channel width, c is a dimensionless constant of order unity that depends on the sediment sorting, g is the gravitational acceleration (m^2/s), d is the reference grain size for the sand (mm), and D is the nearly uniform grain size originally used in Bagnold's experiments (250 μm), and u_* is the friction velocity proportion.

The maximum concentration of sediment that float along the channel is calculated by:

$$conc_{sed, ch, mx} = c_{sp} \times v_{ch, pk}^{spexp} \quad (7)$$

where: $conc_{sed, ch, mx}$ is the maximum concentration of sediment (t/m^3), c_{sp} is a coefficient defined by the user, $v_{ch, pk}$ is the peak channel velocity (m/s), and $spexp$ is an exponent factor defined by the user. If the maximum concentration in the stream is lower than the lower concentration at the inlet of each stream segment, the deposition is dominant. Otherwise, if the degradation process is governed by the segment, it is assumed that the maximum concentration in the channel is greater than the initial concentration. Equations 8 and 9 enable to estimate the maximum deposited and degraded sediment concentrations that can be produced in channels.

$$sed_{dep} = (conc_{sed, ch, i} - conc_{sed, mx}) V_{ch} \quad (8)$$

where: sed_{dep} is the amount of sediment deposition (metric tons), $conc_{sed, ch, j}$ is the initial sediment concentration (ton/m^3), $conc_{sed, mx}$ is the maximum of sediment concentration traveling along the channel (ton/m^3), and V_{ch} is the volume of water in channel (m^3)

$$sed_{deg} = (conc_{sed, ch, mx} - conc_{sed, ch, i}) V_{ch} K_{CH} C_{CH} \quad (9)$$

where: sed_{deg} is the amount of sediment re-entrained in the reach segment (metric tons), $conc_{sed, ch, mx}$ is the maximum concentration traveling along the channel (ton/m^3), V_{ch} is the volume of water in channel (m^3), K_{CH} is the channel erodibility factor ($cm/h/Pa$), and C_{CH} is the channel cover factor.

2.4 Model Calibration and Validation

Having established all required data and parameters, the paired catchment approach was utilized to model the basin, as there were no precipitation gauges available. The energy balance of evaporation from open water surfaces was estimated using the Penman-Monteith method. Additionally, the Muskingum method was utilized in routing the channel flow to calculate surface runoff. The stream power was factored into soil erosion calculations to determine suspended sediment concentration and to predict the location of eroded or deposited river banks. The current study utilized daily time intervals to plot a hydrograph that displays water streamflow, as depicted in Figure 6, for the purpose of modeling predictions. The calibration phase started from 2014 to 2015, followed by validation from 2016 to 2018. Before evaluating the model, a two-year warm-up period was introduced to account for soil moisture content.

2.5 Post-Fire Parameter Adjustment

In this study, the burned area focused only on the forest area. The effect of wildfires on streamflow, erosion rate, and sediment delivery was simulated in conjunction with the fire conditions described by Basso et al. (2019) [8]. The modified parameters were assessed under the following conditions:

- The Curve Number (CN) is used to estimate runoff in relation to cumulative precipitation, soil cover, land use, land cover, and post-fire area. It is an important parameter that can be adjusted to reflect changes in land cover and soil condition caused by wildfire consequences. The vegetation cover, which acts as a natural sponge, is destroyed, resulting in a higher CN value compared to the pre-wildfire condition. The CN value of forest areas in post-fire condition was increased by 5, 10, and 15 for low, moderate and high severity, respectively.

- The Soil Erodibility Factor (USLE_K) is a critical parameter in the SWAT model, used to evaluate soil susceptibility to erosion caused by runoff and raindrop impact, based on soil properties. Its association with burned areas is crucial for

simulating the impact of wildfire on hydrological processes and water resources. Adjusting K values to reflect changes in land use and land cover caused by wildfire can enhance the accuracy of sediment yield predictions in the affected area. The K-factor was risen by 0.014, 0.015 and 0.016 Mg-ha/MJ·mm for low, moderate and high severity, respectively.

- The crop vegetation factor (USLE_C) is used to reflect the effect of cropping and management practices on soil loss. The destruction of vegetation cover and alterations in vegetation characteristics, such as a decrease in biomass and an increase in the exposed soil area, can lead to a decline in the USLE_C value. The values of low, moderate and high burn severity were subtracted by 0.01, 0.05 and 0.2, respectively.

The change of variables must be specified in the database of the SWAT model based on the level of wildfire severity in order to reconstruct the HRUs characteristics. Updating the above values in the model can improve the accuracy of the water and sediment yield estimation in the burned area.

3. Results and Discussion

3.1 Model Performance

3.1.1 Pre-Fire Conditions

The study focused on the discharge and sediment evaluation. The calibration and validation were performed with respect to the statistical indices as coefficient of determination (R^2) and Nash-Sutcliffe efficiency (NSE). The reliability and accuracy of a hydrologic model can be determined based on these two key variables. Calibration took place between 2014 and 2015, and the

simulated flow was validated between 2016 and 2018. Unfortunately, the observed discharge of station 061302 was unavailable in 2016 and 2018. From the pre-fire results, the NSE values for daily flow calibration of pre-fire conditions were 0.63 at station 061302 and 0.57 at P.14A, respectively, as listed in Table 2. The calibrated period was satisfactory for daily analysis. The R^2 values for the daily validation indicated acceptable results at both gauge stations. The NSE values of validated streamflow were equal to 0.72 at the inlet station, which was considered satisfactory model efficiency, however, the consistency of discharges at P.14A was significantly decreased to 0.48. The uncertainty evaluation is possibly linked to the fluctuations in water consumption due to temporal changes in land use and land cover types (e.g., rice fields, orchards, and other agricultural areas). The increase in cultivated areas can result in modifications of land use and land cover, which subsequently influence the amount of surface runoff, evapotranspiration, and water uptake by vegetation. Furthermore, irrigation systems can alter the flow dynamics within the region by redirecting water from natural watercourses or augmenting the water availability for crop growth. Inadequate weather data such as rainfall, temperature, humidity, wind, and solar radiation may lead to another erroneous climate assessment, resulting in an inefficient runoff evaluation in this study. A negative Nash-Sutcliffe Efficiency (NSE) value, coupled with an R^2 value fairly above zero, indicates that the model captures variation but struggles to reproduce the mean, suggesting some relevance with reality in terms of variation. Further studies could involve exploring modifications to the model parameters with a primary focus on preserving the mean in pre-fire and post-fire scenarios.

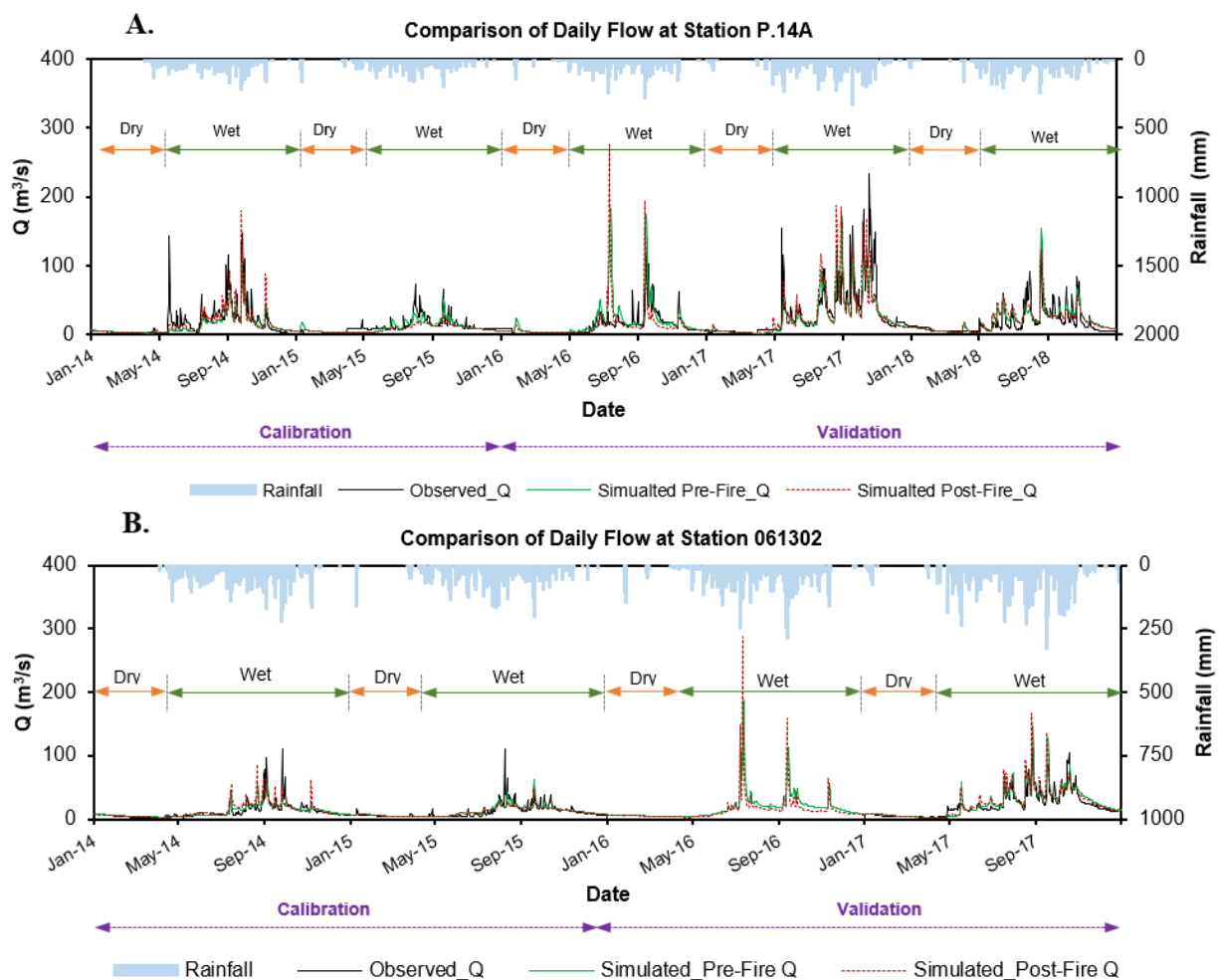


Figure 6. The hydrographs were performed to evaluate the comparison between observed flow data and simulated flow due to pre-fire and post-fire conditions. These comparisons were conducted over both the calibration and verification periods, covering (A.) Station P.14A from 2014 to 2018 and (B.) Station 061302 from 2014 to 2017.

Table 2. The model performance for daily flow and sediment transportation of pre-fire and post-fire conditions and comparison of dry period (January to April) flow rate performance of each year from 2014 to 2018.

Year	Parameters	Station	R ²		NSE	
			pre-fire	post-fire	pre-fire	post-fire
Calibration (Overall) 2014-2015	Q	P.14A	0.60	-	0.57	-
		061302	0.63	-	0.63	-
	SED	061302	0.69	-	0.61	-
Validation (Overall) 2016-2018	Q	P.14A	0.52	-	0.48	-
		061302	0.82	-	0.72	-
	SED	061302	0.86	-	0.46	-
Dry Season 2014	Q	P.14A	0.00	0.22	-0.17	0.15
		061302	0.74	0.75	0.65	0.70
Total-2014	SED	061302	0.67	0.67	0.58	0.52
Dry Season 2015	Q	P.14A	0.04	0.08	-0.93	-0.26
		061302	0.21	0.29	0.11	0.26
Total-2015	SED	061302	0.88	0.68	0.61	0.54
Dry Season 2016	Q	P.14A	0.00	0.01	-2.89	-0.63
		061302	--	--	--	--
Total-2016	SED	061302	0.99	0.99	0.42	0.50
Dry Season 2017	Q	P.14A	0.45	0.53	0.40	0.45
		061302	0.37	0.48	-0.09	0.22
Total-2017	SED	061302	0.67	0.78	0.58	0.72
Dry Season 2018	Q	P.14A	0.43	0.65	0.37	0.66
		061302	--	--	--	--
Total-2018	SED	061302	0.48	0.69	0.07	0.60

-- No observed data available

During the calibration period, the R² and NSE values of sediment transportation were 0.69 and 0.61, respectively. The validated sediment flows provided reliable results with R² = 0.80. However, the efficiency of the model was diminished as indicated by an NSE value of 0.46, as shown in Table 1. Inconsistency in the model can be caused by the incompleteness of observed data over the study period. The observed sediment concentrations were available only at the date of sediment sampling, 67 times from 2014 to 2018. The observed sediment concentration was insufficient over the entire study period due to infrequent sample collection (1-2 times per month). The daily sediment flows at P.14A were primarily predicted throughout the study period.

3.1.2 Post-Fire Conditions

Vegetation recovery typically starts in May, particularly in the middle of the basin where low burn severity has permanently damaged the forest floor. The burned areas were also used to assess streamflow and sediment transport during the dry season from 2014 to 2018. Combining annual burned areas into hydrological models can be hindered by insufficient data, which can constrain the ability to predict sediment concentration during dry periods and prevent a detailed statistical study. Concluding based on a small set of data collected annually during the summer season would not be sufficient to reflect the findings of the study accurately. Consequently, an examination of the fluctuations in annual sediment transport was undertaken.

The statistical indices of inlet and outlet were apparently improved over the pre-fire condition in summer 2017 and 2018, as shown in Figure 7. Results for summer 2017 revealed that R² and NSE statistical values of flow rate estimates at upstream stations (061302) increased from 0.37 to 0.48 and -0.09 to 0.22, respectively. Table 2 shows that the downstream station (P.14A) also showed increases, with R² at 0.53 and NSE at 0.45. The improved results were observed in summer 2018, when adjustments

in the burned areas led to increases in R² and NSE indexes from 0.43 to 0.65 and 0.37 to 0.66, respectively. However, the statistical values were not found to have changed significantly during the years 2014 to 2016, particularly the R² and NSE results at station P.14A. There could be several reasons for the degradation of model performance. The NSE value of -0.26 in 2015 indicates the existence of a negative correlation between the simulated and observed data. A negative NSE value indicates poor model performance and that the observed data has less variation than the simulated data. A lack of sufficient observed burned areas from responsible agencies led to a poor interpretation of the burned area. The impacts of burned areas on each catchment can be complex based on aerial patterns and interactions between land use, weather conditions, vegetation diversity, and soil characteristics. These limitations are obstacles to accurately simulate certain modeling processes [8, 25].

Statistical values of simulated discharge were mostly found to be characterised by insignificant changes during the dry periods, with underestimated or overestimated evaluations of streamflow (inconsistent throughout the study period). From the middle of January to the end of March, the observed outflow was collected with the same value of 9.10 m³/s at P.14A (not only the observed data in 2015 but also errors repeatedly found throughout the study period). Inconsistencies between observed and simulated discharges can lead to inaccurate predictions of sediment transportation by not capturing true flow patterns and factors such as land use and weather. Sampling of suspended sediment concentrations is influenced by and subject to fluctuations based on daily water elevation and time at the hydrometric station [25], resulting in a peak of sediment flow in 2016. Otherwise, the R² and NSE values from the calculations were found to lie within an acceptable range for sediment assessment, but the change in sediment pattern was found to be significant, particularly at the peak of the sediment flow, as shown in Figure 8.

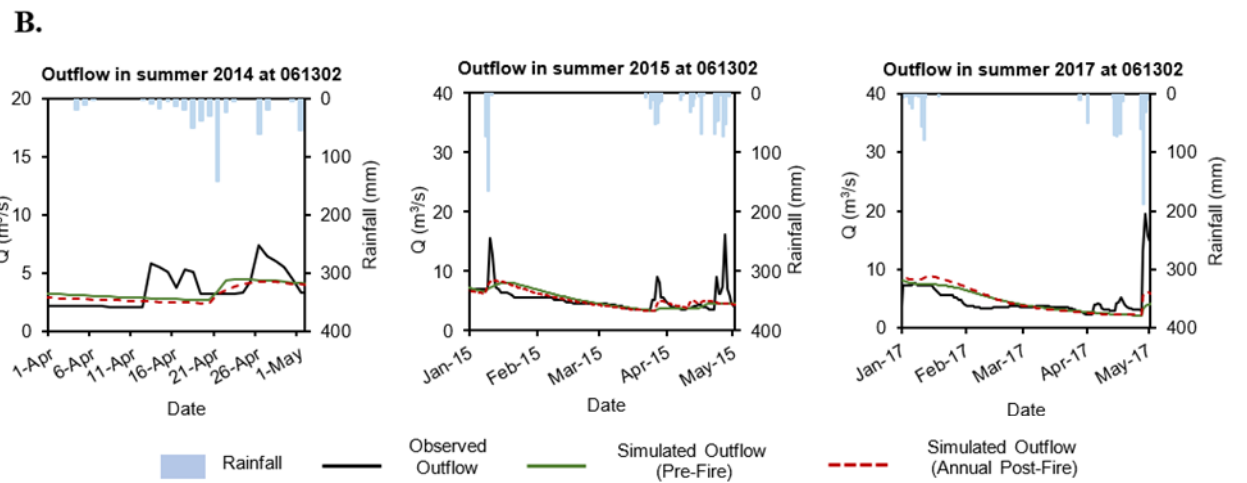
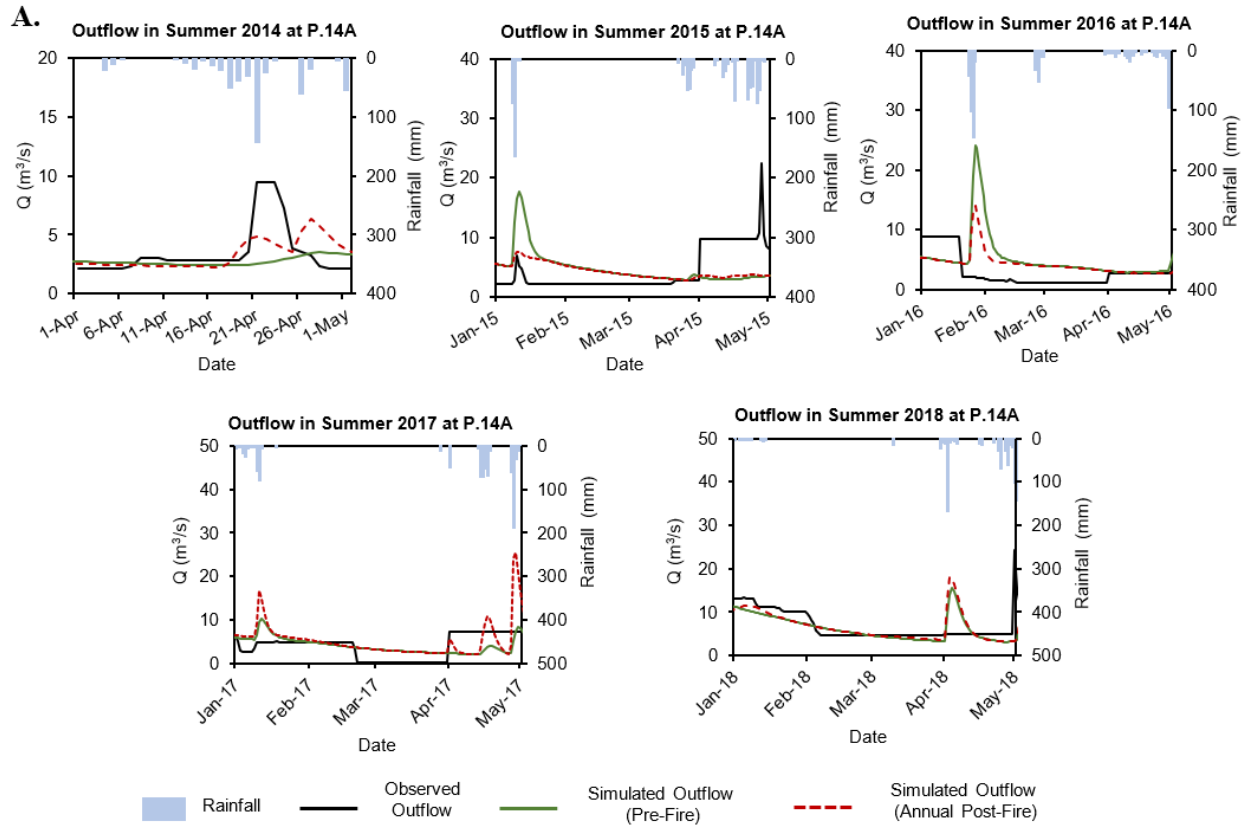


Figure 7. The observed and simulated hydrographic curves compare annual dry season flow rates between pre- and post-fire conditions during calibration and validation periods where is (A) is the basin outlet (P.14A) and (B) is the basin inlet (Station 061302).

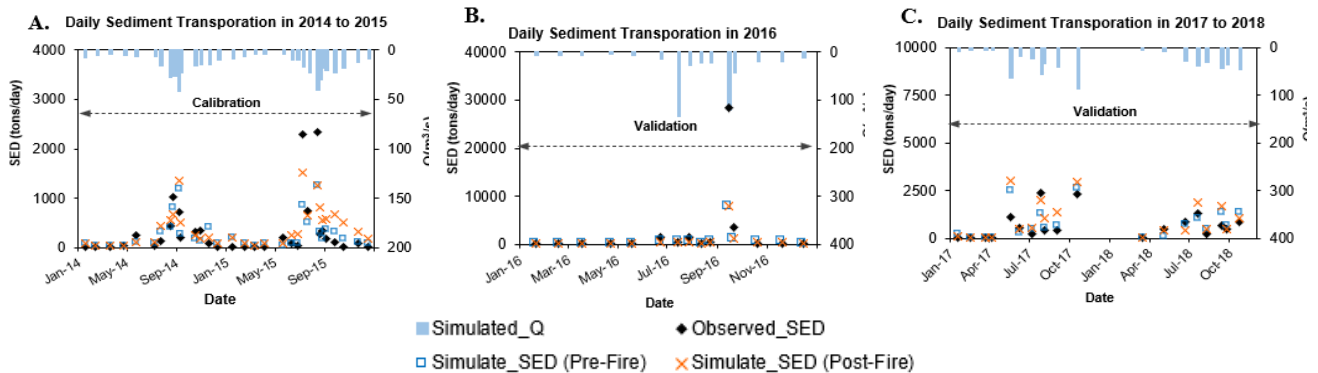


Figure 8. Graph showing daily sediment levels plotted against simulated flow at Station 061302, encompassing data from (A.) the calibrated period, (B.) the validated period in 2016, and (C.) validated period in 2017 to 2018, and contrasting pre-fire and post-fire conditions.

3.2 Wildfire Effect on Streamflow

Surface runoff and baseflow are the two primary components of streamflow [28]. The high flow, also known as surface runoff, is water that excesses from a tributary into the mainstream. The base flow, also known as low flow, is the portion of the streamflow that sustains between rainfall events by delaying subsurface flow at a shallow depth and linking with another stream [29]. Low flow is the flow of a stream during prolonged dry weather for purposes of permit discharge limits. As wildfires occur during the dry season, low-water flows played a relatively important role in this study.

3.2.1 Surface Runoff Characteristics

As expected, wildfire events have the capacity to change characteristics of surface runoff during calibration and validation. The occurrence of wildfires can also have a considerable effect on the temporal and quantitative characteristics of peak flow rates. The notable increase in peak flow was detected during the annual wet periods at sub-basin and basin scales, as shown in Figure 6. Peak flows in wildfire-affected areas are expected to increase by 2-25% compared to pre-fire conditions, according to hydrographs. With the removal of vegetation, precipitation is unable to be intercepted and retained by the canopy, resulting in an immediate runoff into the river, thereby amplifying the peak flow rates [29]. Additionally, it has been observed that an increase in peak flow rates during the annual precipitation period has an adverse effect on the performance of the runoff model under wildfire conditions. This may be attributed to the regeneration and restoration of forested regions following the annual rainfall period.

According to the results of the accumulative surface runoff, the burned areas have rarely had a significant effect on the channel of annual accumulated surface runoff. The fluctuation trend of simulated runoff volume in the SWAT model is presented in Figure 9. The study found that there was a notable increase in annual cumulative runoff of approximately 10% in 2014, 2017, and 2018 at basin scale. Conversely, a significant decrease of 20% was observed in 2015 and 2016 at basin scale. The flow rate at the sub-basin level revealed that the volume of water discharged into streams tends to be incrementally higher, with a slight increase of approximately 7% or 360 m³/s compared to pre-fire conditions. The total volume of

runoff increases after wildfire disturbance, and this variability can be attributed to a variety of factors such as wildfire intensity, proportion of forest burned, climatic conditions, geology, and soil properties of specific location [11].

The runoff volume under wildfire scenarios may be attributed to the presence of low-intensity wildfires and annual precipitation patterns. Despite the high incidence of burning in 2016, the minimum rainfall intensity had an insignificant impact on the flow estimates, as shown in Figure 10, both during the summer and throughout the year at stations 061302 and P.14A. The increase in water volume can be harmful because it can cause devastating flash floods in the downstream floodplain. The higher CN values were applied in the different forest types (evergreen and deciduous forests) based on severity levels. The results of the study indicate that in areas of low burn severity, the optimal CN values tend to be higher than pre-fire conditions as depicted, in Figure 11. Despite the great increase in CN values, total runoff at main stations slightly changed, indicating little impact from the wildfire on water flow. According to the 2017 post-fire results in Figure 8, the runoff volume at P.14A, this was the most affected by the forest fire, increased by approximately 25%. Otherwise, the 2017 burned-scars had little effect on upstream runoff volume, which increased from 4,185 to 5,253 m³/s, or about 8%. The highest CN value adjusted in 2017 is also directly related to the maximum rainfall intensity inundating the basin, as illustrated in Figure 11. This suggests that runoff is a small contributor to rainfall in low-level severity areas. According to Figure 11, most CN values are on the rise and fall between 52 to 84. However, the data still exhibits significant variability and fluctuation from one year to the next. The inadequacy of the CN value makes optimization of burned areas in typical areas extremely difficult. Even in undisturbed forest conditions, determining correct curve numbers in forested watersheds is difficult because the diverse land covers were induced by varying severity, intensity, and fire recurrence [28]. The Curve Number (SCS-CN) should be applied in the field to improve the limitations of the hydrological model [29]. In addition, the initiation of regeneration for various tree species may occur at different times. The impact of wildfires on vegetation and soil may be mitigated through the process of tree regeneration.

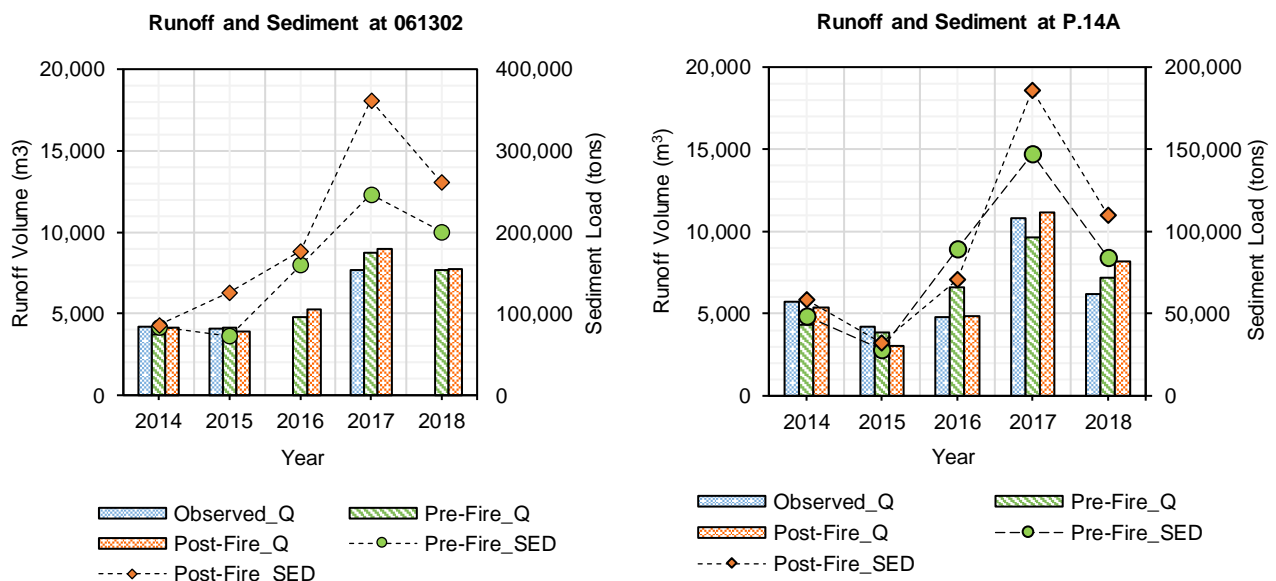


Figure 9. The bar graphs of annual runoff are plotted together with the scatter graphs of cumulative sediment transported and discharged from (A.) Station 061302 and (B.) Station 061302. P.14A, respectively.

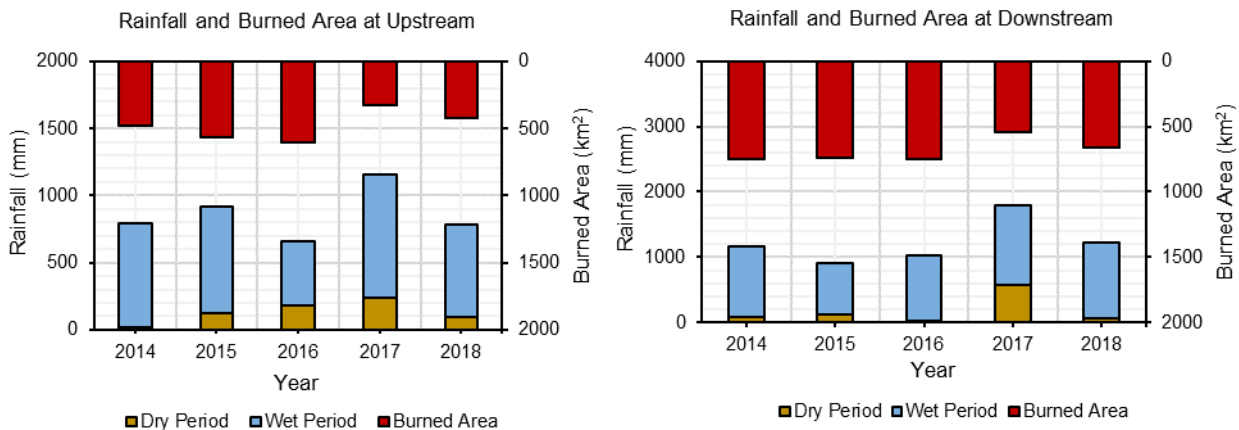


Figure 10. Graph showing comparison between annual rainfall intensity and the proportion of burned areas in two watershed regions, the upstream basin (1st to 5th sub-basins) and the downstream basin (6th to 12th subbasins).

The runoff volume under wildfire scenarios may be attributed to the presence of low-intensity wildfires and annual precipitation patterns. Despite the high incidence of burning in 2016, the minimum rainfall intensity had an insignificant impact on the flow estimates, as shown in Figure 10, both during the summer and throughout the year at stations 061302 and P.14A. The increase in water volume can be harmful because it can cause devastating flash floods in the downstream floodplain. The higher CN values were applied in the different forest types (evergreen and deciduous forests) based on severity levels. The results of the study indicate that in areas of low burn severity, the optimal CN values tend to be higher than pre-fire conditions as depicted, in Figure 11. Despite the great increase in CN values, total runoff at main stations slightly changed, indicating little impact from the wildfire on water flow. According to the 2017 post-fire results in Figure 8, the runoff volume at P.14A, this was the most affected by the forest fire, increased by approximately 25%. Otherwise, the 2017 burned-scars had little effect on upstream runoff volume, which increased from 4,185 to 5,253 m³/s, or about 8%. The highest CN value adjusted in 2017 is also directly related to the maximum rainfall intensity inundating the basin, as illustrated in Figure 11. This suggests that runoff is a small contributor to rainfall in low-level severity areas. According to Figure 11, most CN values are on the rise and fall between 52 to 84. However, the data still exhibits significant variability and fluctuation from one year to the next. The inadequacy of the CN value makes optimization of burned areas in typical areas extremely difficult. Even in undisturbed forest conditions, determining correct curve numbers in forested watersheds is difficult because the diverse land covers were induced by varying severity, intensity, and fire reoccurrence [28]. The Curve Number (SCS-CN) should be applied in the field to improve the limitations of the hydrological model [29]. In addition, the initiation of regeneration for various tree species may occur at different times. The impact of wildfires on vegetation and soil may be mitigated through the process of tree regeneration.

3.2.2 Baseflow Characteristics

In a watershed, the movement of water is characterized by streamflow, surface flow, and baseflow, which are all interrelated. Baseflow denotes the water that originates from subsurface sources, such as groundwater, and also contributes to streamflow. Wildfires have the capacity to modify the fraction of precipitation that percolates into the subsurface. Wildfires affect hydrology by altering water availability and timing, as well as reducing low-flow conditions. Flow duration curve analysis can reveal changes in flow magnitude before and after a wildfire.

In the present study, baseflow is defined as that flow that is exceeded for greater than 70% of the time. An analysis of the pre-fire hydrological conditions was conducted from 2014 to

2018, and the minimum low-flow conditions were determined to be 2.05 m³/s and 2.16 m³/s at stations P.14A and 061302, respectively. Based on Figures 12-13, the minimum flow rate on the y-axis of the post-fire model was found to be 2.04 m³/s upstream and 2.18 m³/s downstream, indicating that these stations were minimally affected by forest burning, respectively. The average baseflow at the watershed level remained unchanged, with a slight increase from 3.85 to 3.96 m³/s. However, the average low-flow of the post-fire condition decreased by about 0.18 m³/s at station 061302. Inconsistent results across years may impact the understanding of wildfire interactions. Many previous studies have interestingly found that the wildfire decreased baseflow recession rates and were a significant factor in controlling groundwater storage [30-32]. However, several studies have revealed that the fundamental current of baseflow can increase from the pre-fire condition [33].

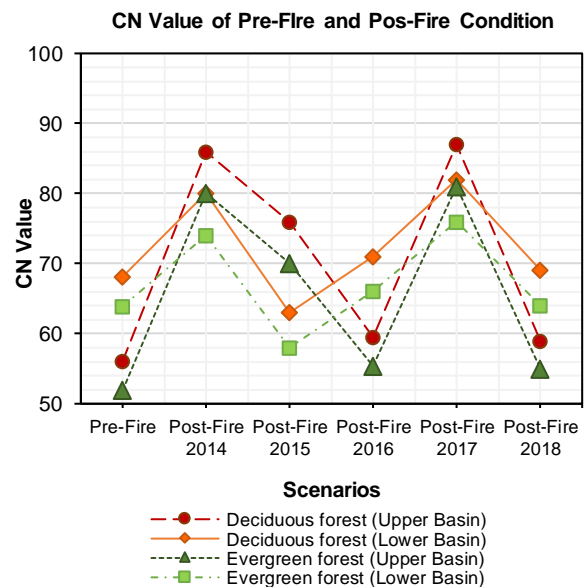


Figure 11. Graph showing the average optimal CN value for forest areas under different model conditions, which includes pre-fire and post-fire conditions, calculated from 2014 to 2018.

The magnitude of average low-flow trends to be lower than the fire event at the subbasin scale, according to post-fire modeling calculations. In the post-fire of Figure 12, there is a slight decrease in the average low-flow, with a decrease of about 8% in 2014, 2016, and 2018. Additionally, the average decrease in the post-fire period is 0.39 m³/s compared to the pre-fire period. The decrease in average low-flow in the post-fire period may be

caused by the damage to the ecosystem from the fire event, leading to a reduction in available water resources and a decrease in the average low-flow. The burning of vegetation and alteration of soil structure during a wildfire can impede the infiltration of precipitation, resulting in diminished availability of water to recharge aquifers and sustain baseflow [29-31]. In contrast, the average low-flow for post-fire modeling at P.14A has increased slightly, particularly from 2016 to 2018, with an approximate increase of 0.26 m³/s or around 5.5% on average, as shown in Figure 13. Wildfires may, in some circumstances, augment low-flow in a stream or river through the enhancement of water infiltration and recharge of subterranean aquifers, as a result of an alteration in soil permeability. [34-35]. As the majority of the burned area was classified as low severity, the elimination of invasive plant species through wildfire can foster the resurgence of native vegetation, thereby enhancing water infiltration and retention and consequently augmenting water availability for baseflow. To further investigate the correlation between baseflow and surface runoff, the evapotranspiration rate, infiltration, water

recharge, groundwater storage, and soil properties should be considered to eliminate the uncertainty results [35].

3.3 Wildfire Effect on Sediment

Fires that combusted leaf litter resulted in an augmentation of runoff volume, which had the potential to exacerbate soil erosion within the burned watershed. The soil safeguarding, which was contingent upon the level of burn severity and strongly correlated with sediment transportation, has been established as a tenuous relationship between hydrological and sedimentary processes [35]. The spatial scale of the wildfire is particularly important when considering its impact on sediment dynamics in the basin. Despite the importance of evaluating the effects of wildfires on sediment transportation and dynamics within a basin, current sediment monitoring methods are typically limited to upstream stations, thereby lacking data on downstream sediment transport. This study sought to fill the gap by providing and comparing quantitative information related to the movement and redistribution of sediment in this river with regard to the effect of wildfire.

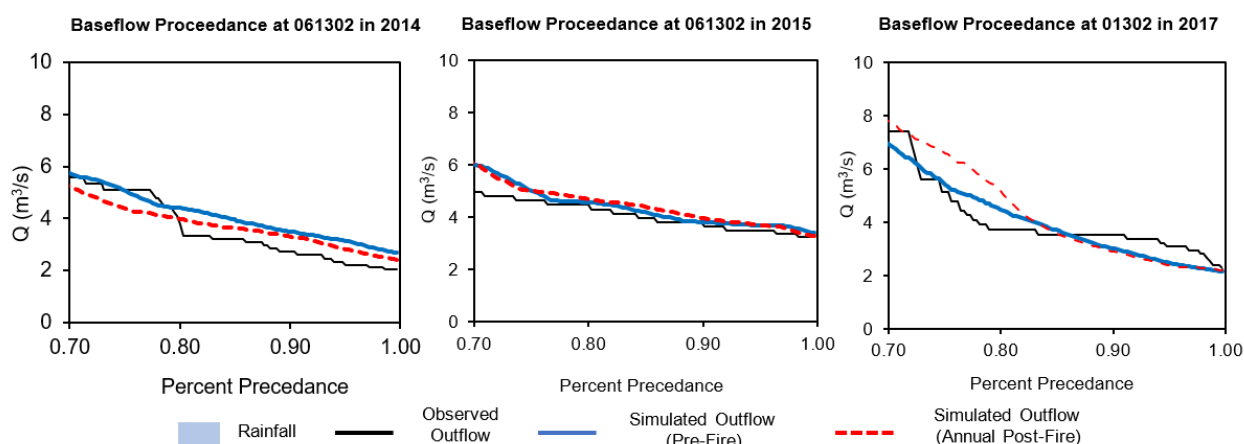


Figure 12. Graph of flow duration curves showing the probability of baseflow occurrence that exceed 70 percent at Station 061302 and comparing observed flow with pre-fire and post-fire conditions.

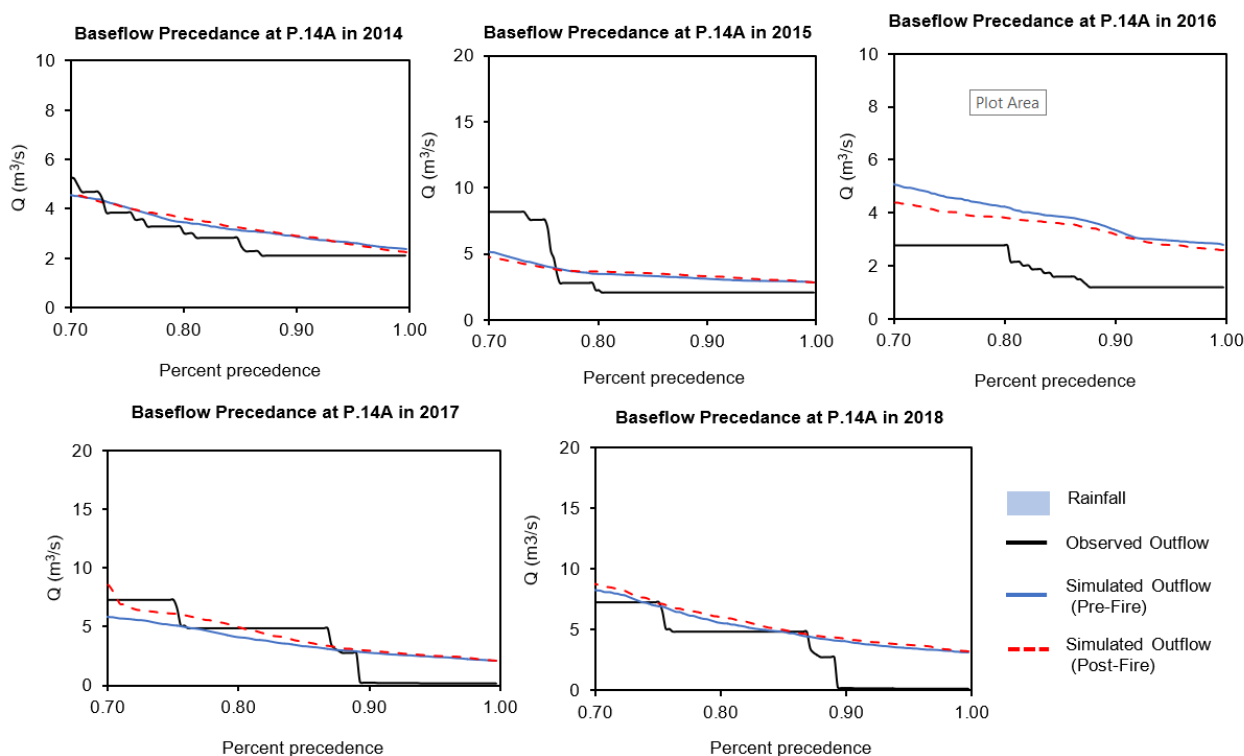


Figure 13. Graph of flow duration curves showing the probability of baseflow occurrence that exceed 70 percent at Station P.14A and comparing observed flow with pre-fire and post-fire conditions.

3.3.1 Sediment Transportation

Low burn severity fires mostly burn the surface vegetation and leave the soil gently damaged, leading to less erosion and sediment transport and faster recovery [36]. The study revealed that a quantity of sediment, approximately 748,450 tons, was transported from station 061302 in pre-fire modelling over the course of the study period. Initially, the upper basin's average sediment yield was computed to be 73.39 t/km²/y. However, the post-fire condition showed that the average sediment yield had significantly risen by 32%, resulting in a new average of 97.33 t/km²/y.

In Figure 9A, the greatest increase in sediment flow is observed in 2015, with a difference of 76,959 tons between post-fire and pre-fire flow, and the second-largest increase is seen in 2017, where the post-fire sediment flow surpasses the pre-fire flow by approximately 115,510 tons. The study showed a strong correlation between changes in flow rates and sediment concentrations following a wildfire, with the peak of sediment flow exceeding pre-fire levels, particularly at station 061302 during the 2015 and 2017 rainy seasons, as shown in Figure 8. The study revealed that 397,164 tons of suspended sediment, or 43.00 t/km²/y, were flowing out of the basin at P.14A due to gravitational forces. Additionally, wildfires have had a significant impact on downstream stations, resulting in an increase in sediment transport rates of approximately 15%, or 49.48 t/km²/y. Furthermore, it can be inferred that the areas downstream (subbasins 6-12) have experienced a substantial loss in sediment yield, potentially indicative of downstream sediment deposition over the period 2014-2018. In most years, the amount of post-fire sediment transportation was higher than the pre-fire amount, ranging from 13.40% to 30.70%. In Figure 9B, a notable increase in sediment transport is observed in 2017, where the post-fire sediment flow surpasses the pre-fire sediment flow by 39,904 tons or 21.04 t/km²/y. The second most significant increase is seen in 2018, where the post-fire sediment flow exceeded the pre-fire sediment flow by 25,893 tons or 14.00 t/km²/y. In 2017, the area of forest that burned the least in the upstream and downstream regions was approximately 323.79 km² and 540.60 km², respectively, as displayed in Figure 10A- 10B. Although, there were fewer burned areas in 2017, it resulted in a greater sediment yield compared to other years, which was attributed to the higher intensity of rainfall [36].

Otherwise, the largest burned area was assessed in 2016, as illustrated in Figure 10B, but the decrease in annual rainfall and surface runoff also had an adverse impact on sludge reduction at P.14A. Sediment transportation decreased by 20.7% compared to the pre-fire condition as shown in Figure 9B. The removal of vegetation by wildfires, which serves as a stabilizing

agent for soil, and the alteration of the landscape, resulting in an increased susceptibility to erosion, can exacerbate the erosion process. Additionally, a decrease in precipitation can also exacerbate erosion by hindering the movement of sediment and soil. The estimation of sediment transportation underneath wildfire events is a complex phenomenon that involves many factors, including land characteristics, precipitation and surface runoff, and the level of burn severity. The inconsistent results that are often obtained in studies may be attributed to variations in these factors, particularly in a heterogeneous environment, where the adapted threshold for classifying the level of burn severity may not be entirely relevant to the actual conditions [4].

3.3.2 Sediment Dynamic

The movement of suspended sediment is primarily controlled by the flow rate and areal characteristics of the sediment supply. Wildfires can have an immediate impact on these factors, altering the movement of sediment particles and the location of erosion and deposition. The Soil and Water Assessment Tool (SWAT) uses a stream power equation to simulate simultaneous sediment degradation and deposition, but this is limited to the mainstream channel only [23]. It means that the patterns of sediment dynamics in tributary streams in subbasins 1, 4, 6 and 9 could not be assessed due to the lower stream order of the hierarchical system in the river.

From Figure 14, the pre-fire modeling predictions indicate that a significant amount of soil particles, around 559,000 tons, were eroded within the river system from 2014 to 2018. Conversely, the capacity for sediment retention within the stream channels was estimated to be approximately 1.9 million tons during the same period. The pre-fire modeling predictions indicated that Channel 3 had the highest amount of soil particles subject to erosion, accounting for 43.75% of total sediment degradation observed from 2014 to 2018. The decrease in sediment loads observed in Figure 12 is due to sediment deposition at segment no. 10, where a significant amount of sediment (537,5480 tons) was discovered to have settled. The downstream deposition of sediment can be attributed to the gradual decrease in water velocity as it transits from the headwater to the downstream, thereby allowing for the sediment particles to be deposited on the riverbed [37]. Within a 5-year period, approaches that include pre- and post-fire data collection are needed to understand the impact of wildfire on sediment dynamics. One-year changes may partially capture the effects of changes in vegetation, land use, and other factors on sediment deposition and erosion. Therefore, assessing sediment in both pre- and post-fire scenarios is crucial for a comprehensive understanding as shown in Figure 14.

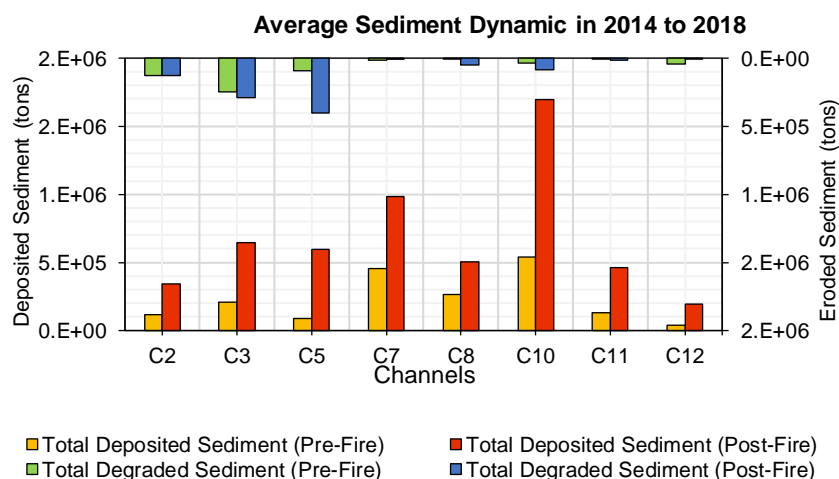


Figure 14. The Bar graph displaying the sediment dynamics in the main channels of the Mae Chaem River, categorized into deposition and degradation processes, from 2014 to 2018.

When compared to pre-fire conditions, the sediment dynamic effects of wildfire disaster reveal a significant increase in sediment degradation, approximately 1.75-fold, as well as a significant increase in sediment deposition, approximately 3-fold. The burned area ratio of 25% or more has a tendency to impact sediment dynamics within the Mae Chaem Basin. The bar graph in Figure 14 shows that the channels in subbasin no. 5 have a higher rate of critical erosion after the fire, due to a higher proportion of burned area (32.37%) compared to the proportion in subbasin no. 3 (24.40%). During 2014-2018, with 1840 mm, the 3rd subbasin of the Mae Chaem Basin had the highest annual precipitation. Intense precipitation can exacerbate soil and sediment erosion, which can be conveyed to downstream areas, resulting in heightened sediment accretion in channels and aquatic environments, thereby potentially diminishing water quality, creating flood hazards, and causing infrastructure damage. There was a significant increase in the total deposited sediment in the post-fire conditions for all channels, and a higher proportion of burned area was associated with a higher increase in deposited sediment. Subbasin 10 continues evidently to be the primary location for sediment deposition, as displayed in Figure 13, similar to pre-fire conditions. Despite this similarity, there has been a marked increase in sediment deposition, totaling 1.16 million tons, due to the highest proportion of burned area at 56.77%, in Figure 15, which covers half of the subbasin's drainage area. This is possibly due to the faster velocity and time compensation of runoff over the same cross-sectional area [13]. The shallowness of the sub-stream can exacerbate the potential for flooding in adjacent regions. The rainfall threshold and proportion of burned area are related to the effective hydrological and sedimentological responses and should be determined further in future work, using more accurate region-specific data. The adjustment of rainfall frequency and intensity after wildfire occurrence should be accounted for in future investigations.

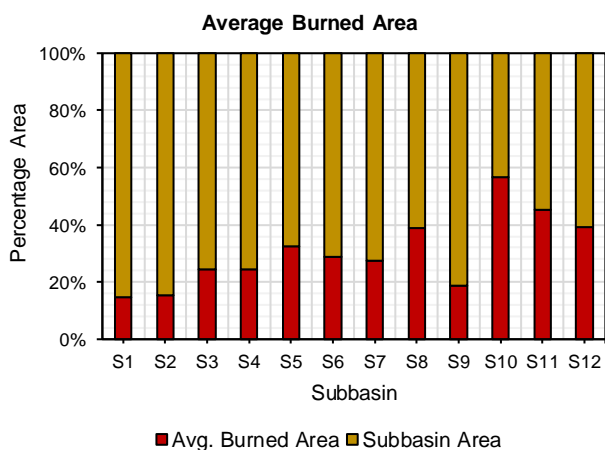


Figure 15. Graph presenting the average of the percentage of burned area and drainage area per sub-basin, calculated from 2014 to 2018. The burned area was evaluated using a dNBR analysis.

4. Conclusions

The present study aimed at quantifying the wildfire-induced perturbations on hydrological and sedimentological regimes through the implementation of distributed modeling as the SWAT model. This study also examined variations in the characteristics of surface runoff, subsurface flow, sediment transport, and sediment dynamics within the Mae Chaem River basin from 2014 to 2018, compared between pre-fire and post-fire conditions. The analysis of the model's performance demonstrated conclusively that the Soil and Water Assessment

Tool (SWAT) model is an efficacious hydrological simulation program for assessing the impact of LULC, soil, and vegetation changes. The analysis of the Difference Normalized Burn Ratio (dNBR) indicated that the dominance of the areas affected by the wildfire indicated a low burn severity, approximately 90% of the total burned area, primarily resulting in the devastation of the vegetation cover and physical properties of the land.

The result showed that the increase in burned land between 2014 and 2018 resulted in a significant acceleration of peak flowrate during wet periods, leading to a substantial enhancement in the annual surface runoff. The study revealed that there was a predominance of annual cumulative runoff at around 10% at the basin scale (P.14A). The consistency of the results was also observed at the station 061302, indicating that the amount of water discharged into streams displayed a slight increase of approximately 7%. A slight decrease in the average baseflow was observed in the upstream basin, with a decline of roughly 0.39 m³/s. On the other hand, post-fire modeling at P.14A revealed a slight increase in the average low-flow rate, registering a 0.26 m³/s increase. These fluctuations should be subjected to further evaluation in order to fully comprehend their effects, and an analysis incorporating factors such as infiltration and evapotranspiration rates should also be conducted.

Changes in sediment transport and sediment dynamics are characterized by a complicated relationship between precipitation intensity, runoff, and the interactions between burned areas. The wildfire events resulted in a significant enhancement of annual sediment transport by 33% (24 t/km²/y) and 15% (6.5 t/km²/y) at stations 061302 and P.14A, respectively. Furthermore, wildfires caused an exacerbation of the sediment transport peaks during the rainy season, which have similar effects as runoff peaks. The proportion of low-severity combustion exceeding 25% has a critical impact on the sediment dynamics within the basin. Wildfire caused a significant 1.75-fold rise in sediment degradation and a substantial 3-fold increase in sediment deposition.

Acknowledgements

This work was supported in part by the Joint Graduate School of Energy and Environment. The hydro-meteorological data was provided by the Thai Meteorological Department, the Royal Irrigation Department, and the Water Resource Regional Office 1, Department of Water Resources. The land use map was supplied by the Land Development Department, Thailand.

References

- [1] Ukrainstev, A.V., Plyusnin, A.M. and Chernyavskii, M.K. 2019. Effect of forest fires on the State of River in Zaigraevkii Raion, the Republic of Buryatia, *Water Resources*, 46(1), 11-18.
- [2] López-Vicente, M., González-Romero, J. and Lucas-Borja, M.E. 2020. Forest fire effects on sediment connectivity in headwater sub-catchments: Evaluation of indices performance, *Science of the Total Environment*, 732, 139206, Available online: <https://doi.org/10.1016/j.scitotenv.2020.139206>.
- [3] Ratchapol, R. 2020. *Chiang Mai Wildfires: Why This Year is Heavier than Every Year*. Available online: <https://www.bbc.com/thai/thailand-52146438> [Accessed on: 20 April 2022].
- [4] Nagler, L.P., Cleverly, J., Glenn, E., Lampkin, D., Huete, A. and Wan, Z. 2005. Predicting riparian evapotranspiration from MODIS vegetation indices and meteorological data, *Remote Sensing of Environment*, 15(1), 17-30.
- [5] Fox, D.M., Laaroussi, Y., Malkinson, L.D., Maselli, F., Andrieu, J., Bottai, L. and Wittenberg, L. 2016. POSTFIRE:

- A model to map forest fire burn scar and estimate runoff and soil erosion risks, *Remote Sensing Applications: Society and Environment*, 4(5), 83-91.
- [6] López-Vicente, M., Poesen, J., Navas, A. and Gaspar, L. 2013. Predicting runoff and sediment connectivity and soil erosion by water for different land use scenarios in the Spanish Pre-Pyrenees, *CATENA*, 102, 67-73.
- [7] Smith, H.G., Sheridan, G.J., Lane, P.N.J., Nynam, P. and Haydon, S. 2011. Wildfire effects on water quality in forest catchments: A review with implications for water supply, *Journal of Hydrology*, 369, 170-192.
- [8] Nunes, J.P., Keesstra, S., Doerr, S. and Pulquério, M. 2018. *Policy Brief: Impacts of Fires on Water Quality*. The Connectur/PLACARD workshop on Fire impacts on water quality, Lisbon, February 2018.
- [9] Basso, M., Vieira, D., Ramos, T.B. and Mateus, M. 2019. Assessing the adequacy of SWAT model to simulate postfire effects on the watershed hydrological regime and water quality, *Land Degradation & Development*, 31, 619-631.
- [10] Olsen, W.H., Wagenbrenner, J.W. and Robichaud, P.R. 2021. Factors affecting connectivity and sediment yields following wildfire and post-fire salvage logging in California's Sierra Nevada, *Hydrological Processes*, 35, 13984, <https://doi.org/10.1002/hyp.13984>.
- [11] Moody, J.A. and Martin, D.A. 2001. Post-fire, rainfall intensity-peak discharge relations for three mountainous watersheds in the Western USA, *Hydrological Processes*, 15(15), 2981-2993.
- [12] Neary, D.G., Gottfried, G.J. and Ffolliott, P.F. 2003. *Post-Wildfire Watershed Flood Responses*. Second International Fires Ecology and Fire Management Congress, Orlando, Florida, November 2003.
- [13] Debano, L.F. 2000. The role of fire and soil heating on water repellency in wildland environments: A review, *Journal of Hydrology*, 231, 195-206.
- [14] Certini, G. 2005. Effects of fire on properties of forest soils: A review, *Oecologia*, 143, 1-10, Available online: <https://doi.org/10.1007/s00442-004-1788-8>.
- [15] Havel, A., Tasdighi, A. and Arabi, M. 2018. Assessing the hydrological response to wildfire in mountainous regions, *Hydrology and Earth System Science*, 22, 2527-2550.
- [16] Ekkawatpanit, C., Kazama, S., Sawamoto, M. and Ranjan, P. 2009 Assessment of water conflict in Mae Chaem River Basin, Northern Thailand, *Water International*, 34, 242-263.
- [17] Climatological Center, Thai Meteorological Department. 2023. *Seasons of Thailand*. Available online: <http://climate.tmd.go.th>.
- [18] Meneses, B.M. 2021. Vegetation recovery patterns in burned areas assessed with landsat 8 OLI imagery and environmental biophysical data, *Fire*, 4, 76, Available online: <https://doi.org/10.3390/fire4040076>.
- [19] Gallagher, M.R., Skowronski, N.S., Lathrop, R.G., McWilliams, T. and Green, E.J. 2019. An improved approach for selecting and validating burn severity indices in forested landscapes, *Canadian Journal of Remote Sensing*, 46, 100-111.
- [20] Rozario, F.P., Madurapperuma, B.D. and Wang, Y. 2018 Remote sensing approach to detect burn severity risk zones in Palo Verde National Park, Costa Rica, *Remote Sensing*, 10, 9, 1427, Available online: <https://doi.org/10.3390/rs10091427>.
- [21] Saputra, A.D., Setiabudidaya, D., Setyawan, D., Khakim, M.Y.K. and Iskandar, I. 2017. Burn scar analysis using normalized burning ratio (NBR) index during 2015 forest fire at Merang Kepahyang peat forest, South Sumatra, Indonesia. *AIP Conference Proceedings*. International Symposium on Earth Hazard and Disaster Mitigation (ISEDMD) 2016: The 6th Annual Symposium on Earthquake and Related Geohazard Research for Disaster Risk Reduction. July 2017.
- [22] Forest Fire Control Division, National Park, Wildlife and Plant Conservation Department, Thailand. 2023. Wildfire statistics by forest fire control. Available online: <https://portal.dnp.go.th/Content/firednp?contentId=15705>.
- [23] Arnold, J.G., Moriai, D.N., Gassma, P.W., Abbaspour, K.C. White, M.J., Srinivasan, R., Santhi, C., Harmel, R.D., van Griensven, A., van Griensven, M.W., Kannan, N. and Jha, M.K. 2012. SWAT: model use, calibration, and validation, *American Society of Agricultural and Biological Engineers*, 55, 1461-1508.
- [24] Rai, R.K., Singh, V.P. and Upadhyay, A. 2017. *Planning and Evaluation of Irrigation Projects Methods and Implementation*, Elsevier Inc, Amsterdam, Netherland.
- [25] McCuen, R.H., 1941. *A Guide to Hydrologic Analysis using SCS Methods*. Englewood Cliffs, N.J: Prentice-Hall.
- [26] Dutta, S. and Sen, D. 2017. Application of SWAT model for predicting soil erosion and sediment yield, *Sustainable Water Resources Management*, 4, 447-468.
- [27] Bagnold, R.A. 1941. *The Physics of Blown Sand and Desert Dunes*. Methuen & Co., London, England.
- [28] Waterman, B.R., Alcantar, G., Thomas, S.G. and Kirk, M.F. 2022. Spatiotemporal variation in runoff and baseflow in watersheds located across a regional precipitation gradient, *Journal of Hydrology: Regional Studies*, 41, 101071, Available online: <https://doi.org/10.1016/j.ejrh.2022.101071>.
- [29] Price, K. 2011. Effects of watershed topography, soils, land use, and climate on baseflow hydrology in humid regions: A review, *Progress in Physical Geography*, 35(4), 465-492.
- [30] Bart, R.R. and Tague, C.L. 2017. The impact of wildfire on baseflow recession rates in California, *Hydrological Processes*, 31(8), 1662-1673.
- [31] Kinoshita, A.M. and Hogue, T.S. 2011. Spatial and temporal controls on post-fire hydrologic recovery in Southern California watersheds, *Catena*, 87(2), 240-252.
- [32] Kinoshita, A.M. and Hogue, T.S. 2015. Increased dry season water yield in burned watersheds in Southern California, *Environmental Research Letters*, 10, 1403, DOI 10.1088/1748-9326/10/1/014003.
- [33] Bart, R. and Hope, A. 2014. Inter-seasonal variability in baseflow recession rates: The role of aquifer antecedent storage in central California watersheds, *Journal of Hydrology*, 519(A), 205-213.
- [34] Rumsey, C.A., Miller, M.P., Susong, D.D., Tillman, F.D. and Anning D.W. 2015. Regional scale estimates of baseflow and factors influencing baseflow in the Upper Colorado River Basin, *Journal of Hydrology: Regional Studies*, 4(B), 91-107.
- [35] Benavides-Solorio, S.J. and MacDonald, L.H. 2001. Post-fire runoff and erosion from simulated rainfall on small plots, Colorado Front, Range, *Hydrological Process*, 16(15), 2931-2952.
- [36] Meng, X., Zhu, Y., Yin, M. and Liu, D. 2021. The impact of land use and rainfall patterns on the soil loss of the hillslope, *Scientific Reports*, 11, 16341, Available online: <https://doi.org/10.1038/s41598-021-95819-5>.
- [37] Verduyck, K., Grabowski, R.C. and Rickson, R.J. 2017. Suspended sediment transport dynamics in rivers: Multi-scale drivers of temporal variation, *Earth-Science Reviews*, 166, 38-52.